

Retrieval of Particulate Exchanges over Semiarid Ecosystems Based on a Doppler Lidar Methodology

Jesús Abril-Gago^(a,b), Pablo Ortiz-Amezcuca^(a,b), Andrew S. Kowalski^(a,b), Juan Antonio Bravo-Aranda^(a,b), María José Granados-Muñoz^(a,b), Juana Andújar-Maqueda^(a,b), Lucas Alados-Arboledas^(a,b), Juan Luis Guerrero-Rascado^(a,b)

^(a) Andalusian Institute for Earth System Research (IISTA), Granada, 18006, Spain

^(b) Department of Applied Physics, University of Granada, Granada, 18071, Spain
jabrilgago@ugr.es

Abstract: Aerosol particle fluxes have hardly been studied with lidar techniques, although they have been largely studied with in-situ instrumentation throughout the last half century. A novel stand-alone methodology for Doppler lidars was developed and applied for the determination of turbulent aerosol particle exchanges, based on the eddy covariance technique. Flux density profiles were calculated and vertical transport velocity profiles were used for the analysis of the particulate exchanges over two distinct Mediterranean dryland ecosystems. Several case studies were examined and notable upward transport velocities were observed during convective regimes and during windy conditions, related to an increase in turbulent activity. Both locations were found to be net sources of aerosol particles during the studied period, although with slightly different average behavior. Footprint analysis confirmed the representativeness of the measurements to their respective ecosystems.

1. Introduction

Drylands consist of regions in our planet characterized by low average annual rainfall and high potential evaporation rates. They encompass deserts, semiarid areas, and dry steppes, constituting approximately 45 to 47% of the Earth's landmass [1]. In Spain, they covered 69% of the total land area in 2011 [2].

Ecosystems exchange energy and matter, encompassing sensible heat, trace gases, and aerosol particles. Traditionally, the eddy covariance (EC) technique has been used to characterize these exchanges, as the covariance between the fluctuations of a scalar and the fluctuations of the vertical wind speed yield the turbulent flux density of the scalar:

$$F_a = \rho \overline{a'w'} \quad (1)$$

where, F_a represents the flux density, ρ denotes air density, a' is the fluctuation of the scalar with respect to its mean (typically a 30-minute average), and w' represents the fluctuation of vertical wind speed about its mean [3].

Aerosol particles constitute a fundamental component of the atmosphere, with influence on cloud formation, radiative forcing, and air quality. Their exchanges depend on wind dynamics, surface roughness and soil surface

[4], and have been extensively quantified across various ecosystems, primarily employing in-situ instrumentation. However, turbulent particle exchanges within semiarid ecosystems have consistently been overlooked [4].

While lidars have been extensively employed to study atmospheric aerosol particles [5, 6], their use in studying particle exchanges has received limited attention. Engelmann and colleagues [7] conducted the first known investigation on aerosol particle fluxes using a combination of Raman and Doppler lidar. However, that study focused on the methodology and provided a calculation of particle fluxes for a singular case under specific conditions. A novel approach to characterize particle fluxes with a sole Doppler lidar is presented in this study.

2. Sites and instrumentation

2.1. Experimental sites

This study took place at two distinct rural stations situated in Southern Spain.

Guadiana (37.91°N, 3.23°W, 370 m asl), is situated inland within an extensive olive grove. The region is characterized by the prevalence of such crops, with a uniform landscape. There are no population centers closer than 5 km and the

station is surrounded by low hills in a radius of 10 km.

Aguamarga (36.94°N, 2.03°W, 205 m asl) is positioned within the heart of Cabo de Gata-Níjar Natural Park (Mediterranean scrub), along the southeastern coast of Spain. The largest population center lies 10 km to the west, while the coast lies 6 km to the east. The landscape is characterized by small hills sparsely covered with a variety of vegetation species.

The aerosol composition at these stations is influenced by local emissions and transport from further regions, as Saharan dust outbreaks. These intrusions carry large loads of particles, which deposit via dry or wet means, exerting a notable impact on soil composition [8].

2.2. Instrumentation and campaigns

A single atmospheric instrument, the HALO Photonics StreamLine XR Doppler lidar, belonging to the ACTRIS AGORA (Andalusian Global ObseRvatory of the Atmosphere) facility, was utilized to measure aerosol particle exchanges. The data were firstly processed using the standardized software package 'Halo lidar toolbox' [9], to retrieve products such as profiles of vertical wind speed (w) and attenuated backscatter coefficient (β_{att}) from 90 m above ground (effective full-overlap height) upwards, with a vertical and temporal resolutions of 30 m and 1 s.

Among the products obtained, special attention is warranted for the profiles of turbulence source classification and Turbulent Kinetic Energy dissipation rate (ϵ) [10]. The first one offers a classification of the main atmospheric mechanisms associated with turbulence. The second one, ϵ , signifies the rate at which turbulence kinetic energy is dissipated into thermal energy. High values of ϵ , exceeding $10^{-4} \text{ m}^2 \text{ s}^{-3}$, indicate large turbulence activity, often associated with convection, while lower values suggest atmospheric stability.

A CHM15k-Nimbus ceilometer (Lufft, Germany) and a Sun-sky photometer (Cimel Electronique, France) integrated into AERONET were co-located, facilitating the interpretation of the particle exchanges. The instrumentation was located in the stations during the campaigns: BLOOM (from May 18 to June 21, 2022, in Guadiana), BLOOM II (from March 28 to May 31, 2023, in Guadiana)

and SCARCE (from July 18, 2023, to January 15, 2024, in Aguamarga).

3. Methodology

The methodology employed in this study was based on that presented by Engelmann and colleagues [7], adapted for a Doppler lidar stand-alone approach. β_{att} , is defined as:

$$\beta_{att}(z) = \beta(z)T^2(z) \quad (2)$$

where $\beta(z)$ represents the volume backscatter coefficient at an altitude z , and $T(z)$ is the transmittance between the instrument and z . $\beta(z)$ describes how much light is scattered backwards and is directly related to the amount of aerosol particles. Thus, $\beta_{att}(z)$ was used as a proxy to compute aerosol particle exchanges as:

$$F_{\beta_{att}}(z) = \overline{\beta_{att}'w'}(z) \quad (3)$$

It is common to normalize these flux densities by the average scalar so that results are easily comparable across studies. Therefore, this study focuses on the vertical transport velocity:

$$v_t(z) = \frac{\overline{\beta_{att}'w'}(z)}{\beta_{att}(z)} \quad (4)$$

generally in cm s^{-1} . The inclusion of the altitude notation, z , is intended to clarify that profiles of v_t are obtained. However, it will be omitted in the subsequent text. Positive values of v_t represent upward particle transport, whereas negative values denote downward transport. Fluxes representativeness assessment was conducted through a flux footprint analysis. The maximum footprint contribution, i.e. the distance between the instrument and the maximum surface contribution to the captured fluxes, was calculated following [11].

4. Results and discussion

During BLOOM, clear skies predominated with occasional middle clouds and some aerosol layers. BLOOM II initially experienced similar atmospheric conditions during an exceptionally dry year, followed by a two-week intense rainfall. SCARCE was characterized by minimal precipitation and clear days. Periods of rainfall were excluded from BLOOM II and SCARCE, aligning with recommendations from the literature to enhance data quality [12].

The prevailing wind patterns during BLOOM and BLOOM II revealed two modes associated with anabatic and katabatic flows. In the case of

SCARCE, two modes aligned with the easterly and westerly wind regimes of the Alboran Sea.

4.1. A clear sky case

Based on ceilometer data (Figure 1a), on April 25, 2023 (BLOOM II), the station experienced cloud-free conditions with low aerosol load confirmed by the Sun-photometer. Analysis of the turbulence source classification (Figure 1b) revealed convection from 8 to 19 UTC, with high values of ϵ throughout the atmospheric column (Figure 1c). Wind shear was identified as the source of turbulence before 6 and after 20 UTC, characterized by lower values of ϵ .

At 8 UTC convection started, turbulence intensified and v_t increased (Figure 1d) showing positive values (upward transport). Positive v_t values propagated upward with boundary layer development. Throughout the day, an average v_t of $(1.2 \pm 2.5) \text{ cm s}^{-1}$ was observed, with a higher value of $(3.2 \pm 3.3) \text{ cm s}^{-1}$ during the convective regime, and negligible upward/downward transport of $(-0.01 \pm 0.48) \text{ cm s}^{-1}$ during the remainder of the period.

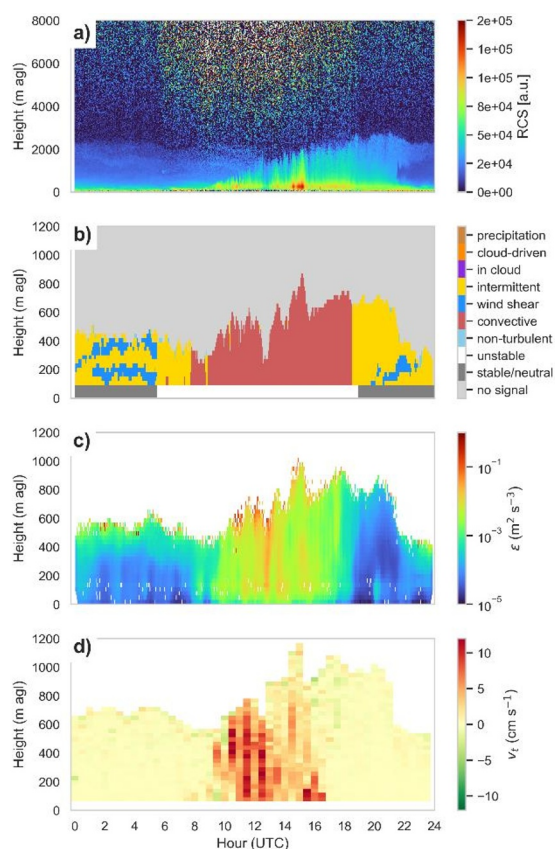


Figure 1. Time series of the vertically resolved a) ceilometer signal (RCS), b) turbulence source classification, c) ϵ and d) v_t over Guadiana on 25 April 2023.

4.2. Campaigns comparison

Figure 2 illustrates the average temporally and vertically resolved v_t for each campaign.

A notable increase in v_t occurs between 6 and 8 UTC, coinciding with the start of convective mixing and boundary layer development. Over time, positive v_t values appear at higher levels, peaking around 12 UTC and reaching around 0.75 km for SCARCE and BLOOM II, and 1 km for BLOOM. BLOOM II exhibits larger v_t levels closer to the surface, potentially due to drier soil conditions. After 14 UTC, positive v_t values diminish both in magnitude and altitude. SCARCE displays a distinct pattern with lower v_t closer to the surface than aloft, from 7 to 18 UTC. This may suggest that convective mixing predominantly drives upward transport during daytime at the inland station (Guadiana), while wind shear may exert greater influence at the coastal station (Aguamarga).

Prior to 6 UTC and after 18 UTC, v_t values notably decrease, aligning with periods of minimal convective mixing and when turbulence primarily arises from wind shear. This decline is more pronounced inland, occasionally even yielding average negative values, whereas the coastal station exhibits lower but positive v_t .

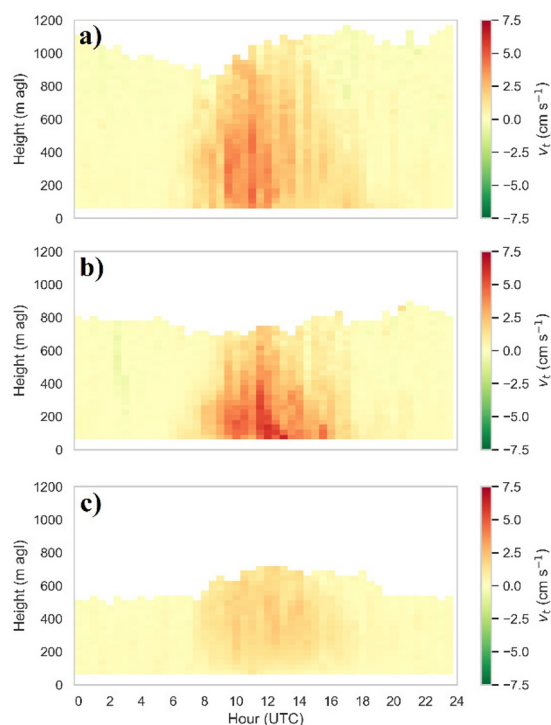


Figure 2. Time series of the vertically resolved average v_t for a) BLOOM, b) BLOOM II and c) SCARCE.

The focus of the study now shifts to the lowermost height interval, from 90 to 120 m, providing the most representative data of ecosystem exchanges. At this altitude, BLOOM and BLOOM II demonstrate an average v_t of (1.1 ± 2.5) and (1.5 ± 4.9) cm s^{-1} , respectively, with 73% and 70% of periods indicating upward transport. SCARCE registers an average v_t of (0.2 ± 1.6) cm s^{-1} , with 58% of periods indicating particle emissions. Both dryland stations appear to act as sources of aerosol particles, though Aguamarga displays lower emissions compared to Guadiana.

To assess the representativeness of the fluxes between 90 and 120 m, flux footprints were analyzed. In Guadiana, instability and stability scenarios were analyzed, yielding the maximum footprint contributions at 350 m and 750 m upwind, respectively. In Aguamarga, easterly and westerly wind patterns were considered. Both exhibited the maximum footprint contributions at around 470 m for unstable regimes, while the stable regimes presented the maximum footprint contributions often exceeding 1 km (still within the Natural Park). Thus, footprint analyses indicated that the particle fluxes detected in the lower range correspond to the studied ecosystems, as land use is uniform within the maximum contribution area. Examinations at higher altitudes revealed an increase in the maximum footprint contribution location.

5. Conclusions

A novel methodology for retrieving aerosol particle fluxes using Doppler lidars was introduced and implemented across three distinct campaigns in Southern Spain.

An illustrative clear-sky day characterized by convection was presented, revealing that convective mixing served as primary driver for the upward transport of aerosol particles.

In average terms, during convective regimes and even nocturnal hours, a consistent positive trend in v_t was observed at every altitude across all the campaigns, confirming particle emissions over the stations. Non-convective periods exhibited markedly lower v_t .

6. Acknowledgements

This work was supported by the project INTEGRATYON³ (PID2020-117825GB-C21 and PID2020-117825GB-C22) funded by

MCIN/AEI/10.13039/501100011033, project MORADO (C-366-UGR23) funded by Junta de Andalucía, the Cost Action PROBE and a project supported by the EC under the H2020-INFRAIA-2020-1 (grant 101008004). J. Abril-Gago received funding from FPU 21/01436.

7. References

- [1] Mirzabaev, A., et al., “Cross-Chapter Paper 3: Deserts, Semiarid Areas and Desertification. In: Climate Change 2022: Impacts, Adaptation and Vulnerability. Contribution of Working Group II to the Sixth Assessment Report of the Intergovernmental Panel on Climate Change”, (Cambridge University Press, Cambridge, UK and New York, NY, USA, 2022), pp. 2195–2231.
- [2] Zdruli, P., “Desertification in the Mediterranean Region”, (European Institute of the Mediterranean, Girona, Barcelona, 2011), pp. 250–255.
- [3] Stull, R. B., “An introduction to boundary layer meteorology”, Springer (1988).
- [4] Webb, N. P., et al., “Size distribution of mineral dust emissions from sparsely vegetated and supply-limited dryland soils”, *J. Geophys. Res. Atmos.*, 126, e2021JD035478 (2021).
- [5] Abril-Gago, J., et al., “Statistical validation of Aeolus L2A particle backscatter coefficient retrievals over ACTRIS/EARLINET stations on the Iberian Peninsula”, *Atmos. Chem. Phys.*, 22, 1425–1451 (2022).
- [6] López-Cayuela, M. Á., et al., “Vertical characterization of fine and coarse dust particles during an intense Saharan dust outbreak over the Iberian Peninsula in springtime 2021”, *Atmos. Chem. Phys.*, 23, 143–161 (2023).
- [7] Engelmann, R., et al., “Lidar Observations of the Vertical Aerosol Flux in the Planetary Boundary Layer”, *J. Atmos. Oceanic Technol.*, 25, 1296–1306 (2008).
- [8] Molinero-García, A., et al., “Provenance fingerprints of atmospheric dust collected at Granada city (Southern Iberian Peninsula). Evidence from quartz grains”, *CATENA*, 208, 105738 (2022).
- [9] Manninen, A. J., “Halo Lidar Toolbox”, Github, https://github.com/manninenaj/HALO_lidar_toolbox (2019).
- [10] Manninen, A. J., et al., “Atmospheric boundary layer classification with Doppler lidar”, *J. Geophys. Res. Atmos.*, 123, 8172–8189 (2018).
- [11] Kljun, N., et al., “A simple two-dimensional parameterisation for Flux Footprint Prediction (FFP)”, *Geosci. Model Dev.*, 8, 3695–3713 (2015).
- [12] Rannik, Ü., et al., “Long-term aerosol particle flux observations. Part I: Uncertainties and time-average statistics”, *Atmos. Environ.*, 43 (21), 3431–3439 (2009).